Check for updates

ChemCatChem

Research Article
doi.org/10.1002/cctc.202400271

Chemistry Europe
European Chemical Societies Publishing

www.chemcatchem.org

Impact of the Potential Dependent Surface Adlayer Composition on the ORR Activity and H_2O_2 Formation on Ru(0001) in Acid Electrolytes

Albert K. Engstfeld,*[a, b] Stephan Beckord,[a] Stefan Fuchs,[a, c] and R. Jürgen Behm[a, d]

Stimulated by the increasing interest in ion adsorption effects on electrocatalytic reactions and by recent more detailed reports on the potential dependent adlayer structures formed on Ru(0001) in pure $HClO_4$ and H_2SO_4 electrolytes, we revisited the oxygen reduction reaction (ORR) on structurally well-defined Ru(0001) single crystal surfaces prepared under ultra-high vacuum conditions. We demonstrate that the complex, potential-dependent activity both for the ORR and for H_2O_2 formation is closely related to potential-dependent changes in the composition and structure of the adlayer. Our results demonstrate the enormous effects adsorbed species can have on the ORR reaction characteristics, either by surface blocking, e.g., by (co-)adsorbed bisulfate species, or by participation in the reaction, e.g., by *H transfer from adsorbed H or OH to O_2. The comparison with results obtained on polycrystalline Ru, which differ significantly from Ru(0001) data, furthermore underlines the importance of using structurally well-defined surfaces as a reference system for future theoretical studies.

Introduction

The oxygen reduction reaction (ORR) taking place at the cathode of a fuel cell is considered to play a major role in the energy loss in such systems.[1] Desirably, the reduction of O_2 proceeds to form H_2O.[2–4] However, an indirect path that involves the formation of hydrogen peroxide (H_2O_2), which can further react to H_2O, is equally possible. Pt is the most active pure elementary metal catalyst for the ORR,[4] and, therefore, also the most intensively studied one for this reaction, including a vast number of studies on well-defined single-crystal model electrodes and Pt-based materials.[1,5–8] Much less is known about the reaction pathways on metals that bind reaction intermediates stronger than Pt. In particular, for these metals, it must be considered that the interaction with the electrolyte and anions in the electrolyte also plays a significant role, which in turn can affect the potential dependent reaction characteristics. One metal that exhibits a strong interaction with electrolytes is Ru.

Numerous previous studies reported on the ORR on polycrystalline Ru (Ru(pc)) electrodes (particles, sheets, etc.) in aqueous acidic[9–13] and alkaline electrolytes.[14–18] An early study by Nekrasov and Krushcheva showed that during the ORR in alkaline electrolyte, part of the current is also related to the formation of H_2O_2.[15] Furthermore, the authors reported that the amount of H_2O_2 depends on the amount of Ru surface oxides formed during high-potential oxidation. Their results were later confirmed by Anastasijivic et al., who also observed similar trends in activity and product formation in acid electrolytes.[12,14] These reports and further studies showed that the relative amount of H_2O_2 increases with increasing overpotential, reaching a maximum between the onset of the ORR and the hydrogen evolution reaction (HER) region.[9,11–15,17] Overall, however, the H_2O_2 yields are only within a few percent but vary with the applied potential.

More fundamental insights were gained from studies on single-crystal electrodes, which can be directly linked to the results of theoretical studies. Most of the existing studies, however, report on the ORR on adatom-modified Ru(0001) electrodes, both experimental[19–23] and theoretical.[22,24–27] However, to the best of our knowledge, there is only a single experimental study by Inoue et al., elucidating in more detail the ORR in O_2 saturated $HClO_4$ on bare Ru(0001) and Ru(10$\bar{1}$1) electrodes (including data on Pt-modified surfaces).[19] The authors illustrate that Ru(10$\bar{1}$1) shows a lower overpotential for the ORR on Ru(0001) and is also more selective for the complete reduction.

[a] A. K. Engstfeld, S. Beckord, S. Fuchs, R. J. Behm
Institute of Surface Chemistry and Catalysis, Ulm University,
D-89069 Ulm, Germany
+49 (0)731 25401
E-mail: albert.engstfeld@uni-ulm.de

[b] A. K. Engstfeld
Present Address: Institute of Electrochemistry, Ulm University,
D-89069 Ulm, Germany

[c] S. Fuchs
Present Address: Helmholtz Institute Ulm (HIU)
Electrochemical Energy Storage
Helmholtzstraße 11, D-89081 Ulm, Germany
and
Karlsruhe Institute of Technology (KIT),
P.O. Box 3640, D-76021 Karlsruhe, Germany

[d] R. J. Behm
Present Address: Institute of Theoretical Chemistry,
D-89081 Ulm, Germany

Supporting information for this article is available on the WWW under https://doi.org/10.1002/cctc.202400271

© 2024 The Authors. ChemCatChem published by Wiley-VCH GmbH. This is an open access article under the terms of the Creative Commons Attribution License, which permits use, distribution and reproduction in any medium, provided the original work is properly cited.

© 2024 The Authors. ChemCatChem published by Wiley-VCH GmbH

To understand the activity and stability of the electrode under reaction conditions, it is helpful to know the potential dependent adlayer composition of the electrode, which can at least approximately be inferred from studies in O_2 free electrolytes.[28–34] Such aspects were, however, only discussed more vividly around the time when the work by Inoue et al. appeared or later.[21,29–32,34–43] Therefore, the mechanistic insights provided in the earlier study on ORR on Ru(0001) of Inoue et al., may not be applicable or accurate to the present day.

Considering these recent results and the potential dependent adlayer models proposed in these studies, we revisited the ORR on Ru(0001) in acid, namely $HClO_4$ and H_2SO_4 electrolytes. In these electrolytes, the Ru(0001) surface is never free from adsorbates.[34,40] Part of the adsorbed hydroxyl (*OH) and bisulfate ($*HSO_4$) is only removed below the equilibrium potential for the HER.[34] Therefore, in contrast to former studies, we also explored the ORR in the HER onset potential region. Even though this potential region has no direct technological relevance, it nevertheless is important for the fundamental understanding of the ORR on Ru(0001) and other strongly binding metals.

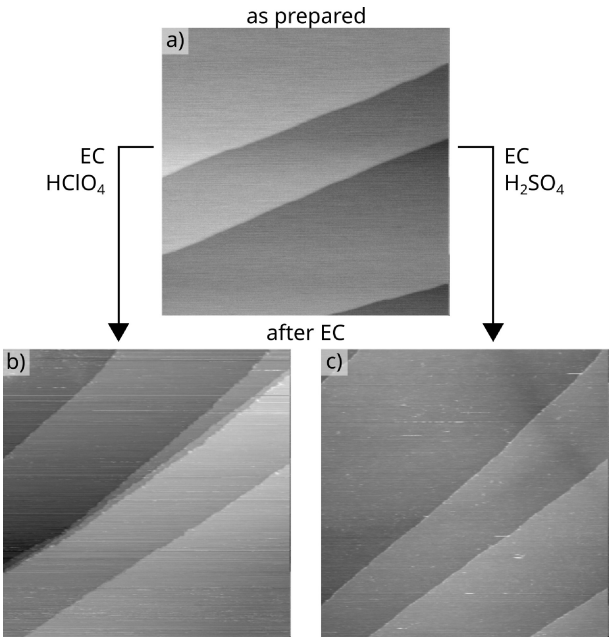

Figure 1. STM images for a Ru(0001) surface recorded a) on an as-prepared surface and after the electrochemical characterization in b) 0.1 M $HClO_4$ and c) 0.5 M H_2SO_4 electrolyte.

Results

Structural Properties

The quality of the electrode surface after the preparation (see Experimental Section) and the stability after the electrocatalytic characterization were verified by scanning tunneling microscopy (STM) measurements under UHV conditions. A representative STM image of the as-prepared surface in Figure a shows extended atomically flat terraces with widths of several 100 nm, separated by monoatomic high and largely straight steps. Images recorded after the electrocatalytic experiments in O_2 saturated 0.1 M $HClO_4$ and 0.5 M H_2SO_4 (Figures 1b and 1c) illustrate that the electrode surface closely resembles the as-prepared surface, without any indications of restructuring.[33]

Electrochemical Properties

The electrochemical properties of Ru(0001) were determined from cyclic voltammograms (CVs), recorded in bare supporting 0.1 M $HClO_4$ and 0.5 M H_2SO_4 electrolytes, which are shown in Figures 2a and 2b (denoted as base CVs – BCVs). The BCVs resemble those reported previously, and a detailed description of the processes within different potential regions or peaks can be found there.[34] Most important for the present work is that certain potential regions are characterized by different adlayer compositions. This is illustrated in Figures 2a and 2b, where the labels I to IV denote the different regions and the suffixes c and a denote the cathodic (negative-going) and anodic (positive-going) scans. More elaborate schematic models of the potential-dependent adlayer, inferred from our previous work,[34] are shown in Figure 3. In summary, region I is characterized by an *O adlayer with a coverage close to 1 monolayer (ML). The * denotes an adsorbed species. In region II, *O is increasingly transformed into *OH.

Starting with the negative-going scan, in $HClO_4$, OH* partially desorbs, leaving about 0.5 monolayers (ML) of *OH on the surface at 0.1 V. At the end of region III, the remaining *OH adlayer is replaced by *H at the peak at 0.0 V. In H_2SO_4, the *OH is first increasingly replaced by adsorbed bisulfate ($*HSO_4$). Note that replacing *OH with $*HSO_4$ can yield a net current of zero (when both species are exchanged one to one). Therefore, other techniques than cyclic voltammetry are required to elucidate this process.[34] The mixed *OH (0.3 ML)/$*HSO_4$ adlayer is then replaced by an *H adlayer in the peak at −0.2 V. Region IV is finally dominated by the HER, where the surface is covered by an *H adlayer in both electrolytes.

In the positive-going scan, in the peak at potentials more positive than 0.0 V, adsorbed hydrogen is displaced by *OH in $HClO_4$ or $*HSO_4$ in H_2SO_4 to form anodic molecular hydrogen.[34,38] At potentials more positive than that peak, the processes from the negative-going scan occur in reverse order. Considering the different peak structures in the positive-going scan in this potential region indicates that the potentials for the processes are shifted and that the adlayer composition at a given potential is somewhat different in both scan directions.

ORR – General Aspects

Figures 2c and 2d show the ORR-CVs recorded in O_2 saturated electrolytes at 20 mV s^{-1}. The ORR-CVs were recorded during a sequence of cycles, and subsequent cycles did not show measurable differences, illustrating that the electrodes are stable under these conditions. This conclusion is in line with

© 2024 The Authors. ChemCatChem published by Wiley-VCH GmbH

18673899, 0, Downloaded from https://chemistry-europe.onlinelibrary.wiley.com/doi/10.1002/cctc.202400271 by Karlsruher Institut F., Wiley Online Library on [13/05/2024]. See the Terms and Conditions (https://onlinelibrary.wiley.com/terms-and-conditions) on Wiley Online Library for rules of use; OA articles are governed by the applicable Creative Commons License

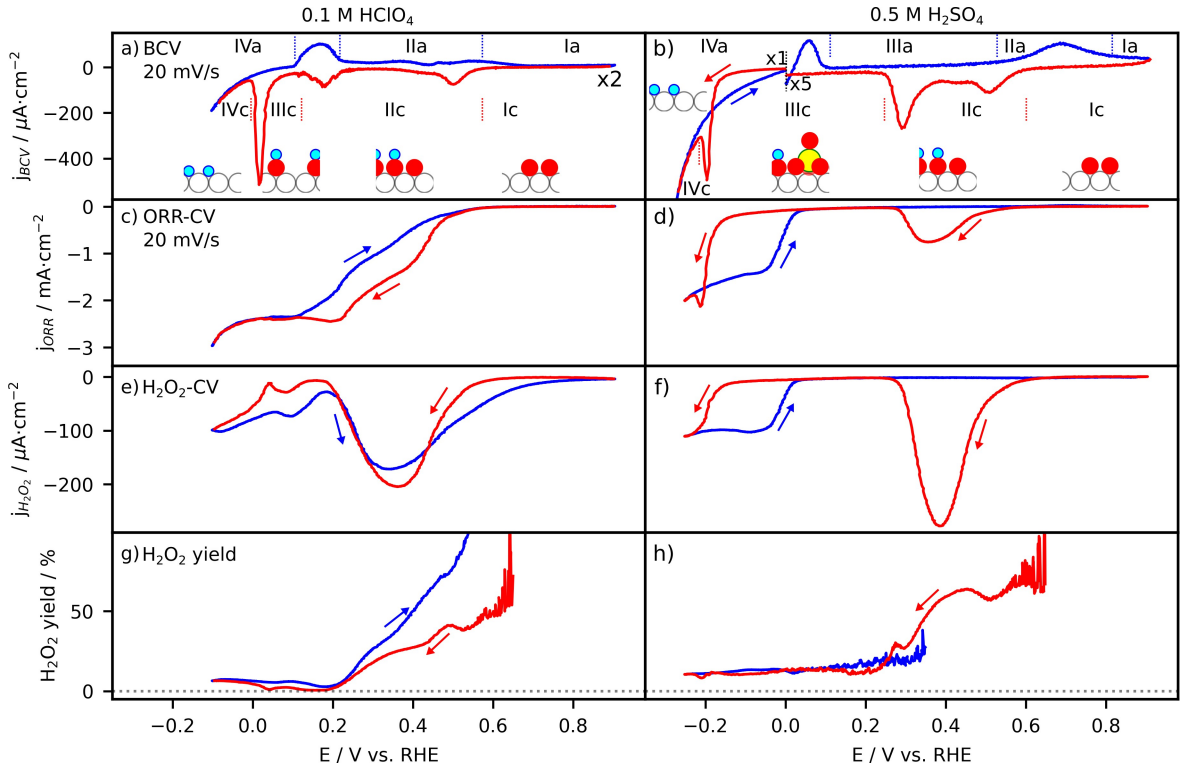

Figure 2. Cyclic voltammograms (CVs) for Ru(0001) recorded at 20 mV s^{-1} in the bare supporting a) 0.1 M $HClO_4$ and b) 0.5 M H_2SO_4 electrolyte denoted as BCV. The BCVs (or certain regions) were rescaled for better visibility of certain features, where the scaling factors are included next to the CVs in the figure. CVs in O_2 saturated electrolytes are shown in c) and d), recorded at 20 mV s^{-1}. Panels e) and f) show the current related to the formation of H_2O_2. This current was determined from the current recorded at the Pt collector electrode, which was held at 1.2 V (see Section S1). The corresponding yields for the formation of H_2O_2 are shown in panels g) and h). The arrows indicate the scan directions, and the negative- (positive-) going scans are plotted in red (blue). Simplified models of the adlayer structures in certain potential regions (denoted by Roman numbers) are added in panels 2a and 2b. More detailed models are depicted in Figure 3.

that derived from the STM images shown in Figure 1, which did not resolve any significant changes after the electrocatalytic measurement. Figures 2e and 2f show the partial currents for the formation of H_2O_2 (H_2O_2-CV), deduced from the currents at the collector electrode. Contributions from the oxidation of H_2 formed on the working electrode at high overpotentials can be excluded (see Section S1 in the SI). This finding agrees with previous works, which showed that the oxidation of H_2 is little efficient on the oxidized Pt collector electrode set at 1.2 V.[44–46] The corresponding H_2O_2 yields are depicted in Figures 2g and 2h. Note that the values obtained very close to the onset potential must be considered cautiously since small variations in the currents on the working and collector electrodes can lead to a strong over- or underestimation of the H_2O_2 yield. Therefore, these data are not included in the plot. The evaluation of the underlying data and their error ranges are described in Section S1 in the SI. Additional pseudo-staircase voltammograms (SCVs), which showed current at selected potentials that were very similar to those obtained in the ORR-CVs, and a comparison of ORR-CVs recorded at different scan rates, illustrate that at most potentials, the measured ORR currents are not affected by slower adsorption/desorption processes (see Section S2 of the SI).

ORR in $HClO_4$

Starting with the ORR-CV for Ru(0001) recorded in 0.1 M $HClO_4$, the onset potential for the ORR in the negative-going scan is located at slightly more positive values than that of the surface reduction processes observed in the BCV. This is shown more clearly in Section S3 of the SI, where the low current region of the ORR-CV is plotted on top of the BCV. Hence, close to the onset potential, the ORR proceeds on the largely *O-covered surface, possibly containing small amounts of *OH. Continuing with the negative scan, the ORR current increases steadily in the range between the onset and about 0.2 V. From this potential, the current is almost constant until the end of region IIc and throughout region IIIc. Apparently, the substantial changes in the adlayer composition in this potential range are hardly reflected in the ORR current. Finally, the ORR current increases again in the HER region IVc. This latter increase in the ORR current also contains contributions from the HER. The contribution is, however, small, based on the current measured in the BCV at the lower potential limit (150 μA cm^{-2}). Note that the ORR on Ru(0001) is not transport-limited,[12,19] which is consistent with our conclusion that the dominant contribution to the increase in current in this potential range originates from the ORR kinetics.

© 2024 The Authors. ChemCatChem published by Wiley-VCH GmbH

18673899, 0, Downloaded from https://chemistry-europe.onlinelibrary.wiley.com/doi/10.1002/cctc.202400271 by Karlsruher Institut F., Wiley Online Library on [13/05/2024]. See the Terms and Conditions (https://onlinelibrary.wiley.com/terms-and-conditions) on Wiley Online Library for rules of use; OA articles are governed by the applicable Creative Commons License

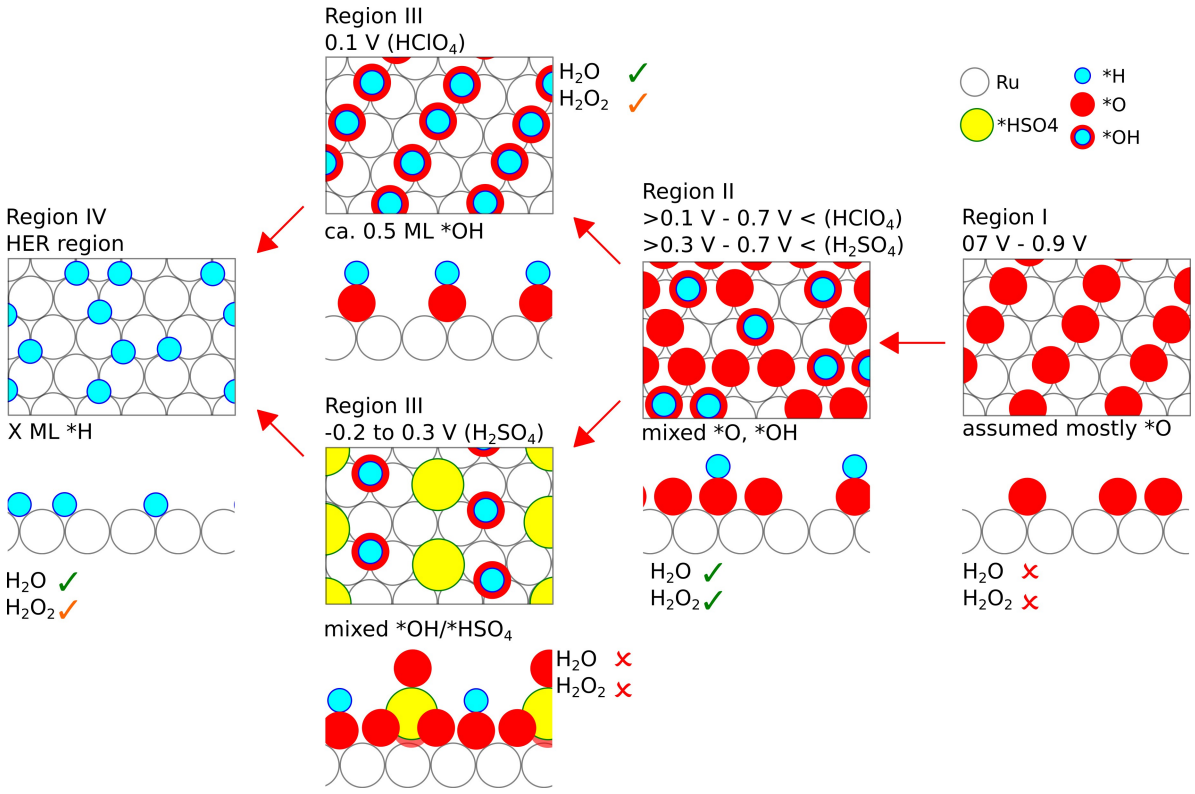

Figure 3. Detailed potential dependent surface adlayer model to that shown in Figure 2, for the negative-going scan during the ORR on Ru(0001) in $HClO_4$ and H_2SO_4. The framed models show a top-down view, and below a cross-section. The checkmarks and crosses next to the individual panels indicate whether or not the ORR proceeds to form H_2O, H_2O_2, or both on the respective surfaces. See text for details. The model was inferred from that presented in Ref. [34].

In the positive-going scan, the current largely follows the previous scan, except for a hysteresis in regions IIIa and IIa, in the range between 0.1 V and the onset of the ORR at 0.6 V, where the cathodic current starts to decrease earlier than in the negative-going scan. A similar behavior was also reported by Inoue et al..[19] In contrast to their data, our ORR-CVs contain a few wavelike structures in the increasing/decreasing ORR current that seem to be correlated with the redox features in the BCV in Figure 2a. Based on our own previous measurements, we suggest that the difference between the two studies is probably related to the surface preparation, i.e., to a higher defect density of the Ru(0001) surfaces used in the former study, the way how the electrochemical measurements were performed, and the design of the electrochemical cell.

The hysteresis in the potential region between 0.1 V and the onset of the ORR is likely related to the different adlayer compositions on Ru(0001) in both scan directions shown previously.[34] We suggest that the hysteresis is similar in O_2 free electrolyte (Figure 2a) and most likely also in O_2 containing electrolyte. Different from the negative-going scan, the *H adlayer extends in the positive-going scan up to the peak centered at 0.15 V (Figure 2a, region IIIa, BCV), where anodic H_2 is formed upon the adsorption of *OH in the BCV.[34] Preliminary differential electrochemical mass spectrometry (DEMS) measurements, which allow monitoring the formation of volatile species in the electrolyte, suggest that anodic H_2 also forms in the presence of O_2 during the ORR (see Section S3). Continuing the positive-going scan, the ORR ceases at the end of region IIa, with the formation of a dense *O adlayer.

H_2O_2 Formation in $HClO_4$

The H_2O_2 in Figure 2e, does not follow the the ORR-CV in Figure 2c. Instead, the H_2O_2 formation starts in the negative-going scan with the onset of the ORR at 0.6 V and continues in a broad peak, where the approximately 1 ML *O adlayer transforms into a mixed *O/*OH adlayer (see Figure 3).[34] The H_2O_2 formation is almost suppressed at about 0.15 V (end of region IIc), where the surface is covered by about 0.5 ML *OH. The negligible activity remains throughout region IIIc (see Figure 2e). Apparently, the *OH coverage is too low to support H_2O_2 formation despite considerable ORR activity in this region.

With further decreasing potential, the H_2O_2 current then increases again slowly. A more detailed inspection resolves an additional minimum in this region, which seems to coincide with the sharp peak at about 0.0 V (between regions IIIc and IVc in the BCV). In this peak, the remaining *OH is reductively removed from the surface, concomitant with the adsorption of atomic hydrogen (*H) and the onset of the HER. The increasing presence of *H species activates slow H_2O_2 formation down to the lower potential limit.

In the positive-going scan, the amount of H_2O_2 formation decreases reversibly towards more positive potentials for the

© 2024 The Authors. ChemCatChem published by Wiley-VCH GmbH

18673899, 0, Downloaded from https://chemistry-europe.onlinelibrary.wiley.com/doi/10.1002/cctc.202400271 by Karlsruher Institut F., Wiley Online Library on [13/05/2024]. See the Terms and Conditions (https://onlinelibrary.wiley.com/terms-and-conditions) on Wiley Online Library for rules of use; OA articles are governed by the applicable Creative Commons License

same reasons as the increase in the negative-going scan in this region. Interestingly, at the potential where the small minimum in the H_2O_2 formation current was observed in the negative-going scan, now a similar size maximum appears, which is also shifted to more positive potentials (0.1 V). Similar to the behavior in the negative-going scan, the ORR current is almost constant in this potential region. In this region, the BCV also does not show any noteworthy features. Hence, possible adlayer changes are too small to result in detectable currents in the BCV or do not involve a charge transfer. At potentials more positive than 0.2 V, a similar sized peak as in the negative-going scan is observed, whose maximum is also about at 0.3 V. Hence, the H_2O_2 formation increases again with increasing *OH coverage in region IIa. The fact that the maximum of this peak is about in the middle of region II indicates that it results from a combination of two effects: (i) an increasing ORR activity with more cathodic potentials and (ii) an optimum composition of this *OH/*O adlayer. Note that the peak reaches far into the potential range of region Ia, consisting of an *OH and *O adlayer, where the ORR currents are negligible (Figure S5). This effect is possibly caused by the large amounts of H_2O_2 formed in region IIa, where part of it is retained in the electrolyte channel between the working and collector electrodes. This effect is less pronounced for CVs recorded at lower scan rates, as shown in Figure S5.

H_2O_2 Yield in $HClO_4$

The yield for H_2O_2 formation in Figure 2g steadily decreases in the negative-going scan, from approximately 60% close to the onset of the ORR to a few percent at around 0.2 V and remains this low also in the HER region. In the positive-going scan, the H_2O_2 yield increases almost reversibly in region IIa, with increasing *OH coverage, also reaching approximately 60% close to the onset potential. In total, H_2O_2 is formed mainly in regions where a significant amount of *OH is present on the surface ($>$0.5 ML *OH in region II). Small amounts are also formed when the surface is covered by *H, i.e., in the HER region IV. This conclusion will be corroborated by the ORR characteristics in 0.5 M H_2SO_4 discussed next.

ORR in H_2SO_4

For the ORR on Ru(0001), in O_2 saturated 0.5 M H_2SO_4 the ORR-CV in Figure 2d is more complex. Similar to the ORR in 0.1 M $HClO_4$, the onset potential in the negative-going scan is located at slightly more positive values than that of the surface reduction processes observed in the BCV (see Section S4). Hence, the ORR starts on the largely *O-covered surface in region I, as in $HClO_4$. This current develops into a distinct peak in region IIc in the potential range, where *O is increasingly replaced by *OH. With decreasing potential, the latter is partly replaced by adsorbed bisulfates (*HSO_4), forming a mixed *OH/*HSO_4 adlayer, with the amount of *OH decreasing and that of *HSO_4 increasing with more negative potentials in region IIIc. In this region, the electrode is essentially inactive. The current increases again at the onset of the HER region IV. The onset coincides with the peak at $-$0.2 V in the BCV and is therefore likely caused by the same surface process, i.e., exchange of the mixed *OH/*HSO_4 adlayer by *H.[34] Significant ORR currents are obtained once the surface is mostly covered by *H, but the overall current is smaller than in O_2 saturated $HClO_4$.

In the positive-going scan, the ORR remains active up to about 0.0 V, followed by a rather steep decay. Hence, there is a pronounced hysteresis in the potential region up to about 0.1 V. The almost inhibition of the ORR in the peak centered at about 0.1 V is caused by the adsorption of *HSO_4, which displaces the *H to form anodic H_2.[34] This process was was verified by preliminary DEMS measurements shown in the SI in Section S3. The ORR is also almost inhibited at higher potentials (complete inhibition at 0.4 V, see Figure S7d) in regions IIIa and IIa, where *HSO_4 is gradually replaced by *OH. Complete removal of *HSO_4 and the transformation of *OH into *O, only occurs at potentials larger 0.6 V, hence at about the onset potential for the ORR in the negative-going scan (Figure S7d). The absence of ORR activity in the positive-going scan seems to be specific for Ru(0001) electrodes in H_2SO_4. In comparison, Ru(pc) electrodes show a similar ORR activity in both scan directions in this potential range (see Section S5 in the SI and elsewhere).[11,47]

H_2O_2 Formation in H_2SO_4

Overall, the H_2O_2 formation closely follows the ORR-CV, indicative of a close relation between ORR activity and H_2O_2 formation in the entire potential range. Overall, H_2O_2 formation is much more pronounced in region IIc than in the HER region IV, indicating that the *OH-dominated adlayer in region IIc plays a significant role in the H_2O_2 formation.

H_2O_2 Yield in H_2SO_4

The yield for H_2O_2 in H_2SO_4 solution reveals similar trends as obtained in $HClO_4$, with a steady decrease in the negative-going scan, from approximately 60% close to the onset potential of the ORR to a few percent at around 0.2 V, and remaining this low also in the HER region. The continuous decay is superimposed by a broad peak at about 0.4 V, which coincides with the peaks in the ORR and H_2O_2 currents in Figures 2d and 2f. As indicated already by the smaller ORR peak (Figure 2d) and the larger H_2O_2 current, this peak is more pronounced than the similar peak in the H_2O_2 yield in $HClO_4$ electrolyte. In the positive-going scan, the H_2O_2 yield is very low in the entire potential range up to 0.0 V, i.e., in the range where the electrode is active for the ORR (Figure 2f).

© 2024 The Authors. ChemCatChem published by Wiley-VCH GmbH

18673899, 0, Downloaded from https://chemistry-europe.onlinelibrary.wiley.com/doi/10.1002/cctc.202400271 by Karlsruher Institut F., Wiley Online Library on [13/05/2024]. See the Terms and Conditions (https://onlinelibrary.wiley.com/terms-and-conditions) on Wiley Online Library for rules of use; OA articles are governed by the applicable Creative Commons License

Discussion

Reaction Pathway

Usually, the ORR is described as an inner-sphere electron transfer reaction, where O_2 adsorbs on adjacent, available surface sites and reacts in a multistep reaction with the surface via intermediates such as *OOH or *OH to form either H_2O_2 or H_2O.[4,48,49] From this reaction pathway, and using the concept of linear scaling, it is expected that for metals that bind atomic oxygen strongly, such as Ru, the ORR should predominantly proceed via the four-electron pathway to form H_2O.[4,48,49] As stated already in Ref. [48], this relation might, however, not be applicable for surfaces covered by other adsorbates. In that case, the reaction rate should be zero, even though the bare surface would be active. Moreover, on surfaces partially covered by adsorbates other than reactants or reaction intermediates, the adsorbate-covered sites/areas can contribute via different reaction pathways to the total reaction than those dominant on bare surface sites. Therefore, knowing the surface adlayer composition and coverage is imperative for an in-depth discussion of the respective reaction mechanism.

From our previous study of Ru(0001) in O_2 free electrolytes,[34] it is evident that in the potential region from the onset of the ORR to the HER region, the surface is always at least partly, if not fully covered by adsorbates, as illustrated in Figure 3. Therefore, we suggest that in addition to a reaction pathway involving the adsorption of O_2 directly on the Ru(0001) surface and thus a direct interaction between Ru and O_2, there must be another reaction pathway allowing for ORR also on adsorbate covered surfaces/sites. The first pathway would be limited to the potential regions where *OH is partly removed to form water in $HClO_4$. Such situations can be found near the transition from region II to III and in region III (or vice versa). The second pathway, in contrast, must be possible in potential regions where the adlayer is essentially closed, e.g., at the more positive potentials of region II or in the HER region IV.

While independent of the electrolyte, the *O adlayer present in region I seems to block the surface for the ORR completely. Increasing ORR activity is observed with the conversion of *O into *OH at the beginning of region IIc. The situation of O_2 interacting with an *OH-covered surface closely resembles that obtained for the ORR in an alkaline electrolyte. To explain the pronounced formation of H_2O_2 under these conditions, Ramaswamy and Mukerjee suggested that the reaction occurs via an outer-sphere electron transfer reaction, with O_2 being solvated by an H_2O solvation shell and separated from Ru by *OH.[18,50] Our data fully agree with a picture where the adsorbing O_2 is separated by an *OH adlayer from the metal surface. We speculate that hydrogen from the *OH species is transferred to an O_2 species residing above the *OH in a second layer, forming a weakly adsorbed OOH species as in Eq. (1) (the $^{(*)}$ indicates a weakly adsorbing species). Another H is transferred to generate H_2O_2, where the source for the H can be another H from *OH (Eq. (2)) or a proton from the electrolyte (Eq. (3)).

$$^{*}OH + {}^{(*)}O_2 \rightarrow {}^{*}O + {}^{(*)}OOH \quad (1)$$

$$^{*}OH + {}^{(*)}OOH \rightarrow {}^{*}O + H_2O_2 \quad (2)$$

$$H^+ + e^- + {}^{(*)}OOH \rightarrow H_2O_2 \quad (3)$$

Further reactions with protons may rapidly re-hydrogenate the resulting *O to form a new *OH via Eq. (4).

$$^{*}O + H^+ + e- \rightarrow {}^{*}OH \quad (4)$$

In this region, part of the *OH will possibly also be reduced to H_2O, leaving a free Ru site behind. With more negative potentials, the *OH coverage decreases, decreasing the H_2O_2 yield as well, and the 4-electron process via direct contact of O_2 with the Ru surface becomes more competitive and dominant. To explain the rapidly increasing tendency for the 4-electron process, the reactivity of the bare Ru sites for the latter pathway must be significantly higher than that of the *OH-covered sites, which are responsible for the H_2O_2 formation.

While in $HClO_4$, this combination of two reaction pathways can continue up to the formation of the *H-adlayer in region IVc, this is not possible in H_2SO_4. It is well known from the systems that $^{*}HSO_4$ inhibits or blocks the ORR.[51,52] Interestingly, also on surfaces that have a mixed *OH/$^{*}HSO_4$ adlayer (region III), the ORR is completely inhibited. Apparently, the bulky $^{*}HSO_4$ species inhibit both the 4-electron transfer reaction to H_2O, via the direct interaction between O_2 and Ru electrode, and also the mechanism discussed above for the 2-electron transfer reaction to H_2O_2.

In the HER region, where the surface is usually covered by a dense *H adlayer, the adsorbed *H does not have a significant impact on the ORR, as evident from the continuing and even increasing ORR current in this regime. On the other hand, the *H species also do not seem to play a significant role in the formation of H_2O_2, based on the low yields obtained in that region. Most simply, this can be explained by continuous desorption of H_2 and re-adsorption of hydrogen from H^+, which leaves a chance also for O_2 molecules to directly interact with the Ru(0001) surface in temporarily existing vacancies in the *H-adlayer. Comparing the ORR activity in the HER region of both electrolytes, we observed a lower activity in H_2SO_4 than in $HClO_4$, even though $^{*}HSO_4$ can be excluded in this region. We suggest that the lower activity in H_2SO_4 is caused by electrolyte effects,[51,52] which has to be addressed in a separate work.

Comparison with pc Ru

Finally, we discuss the relevance of our findings derived on Ru(0001) for Ru(pc) electrodes. ORR-CVs and H_2O_2 CVs recorded on such electrodes in the two electrolytes are presented in Figure S8 in the SI (note that in this case, the negative potential limit was slightly more positive than in Figure 2). The CVs closely resemble those reported previously,[9,12,13] with a steady increase of the ORR current with decreasing potential. Independent of the electrolyte and of the scan direction, the H_2O_2

© 2024 The Authors. ChemCatChem published by Wiley-VCH GmbH

18673899, 0, Downloaded from https://chemistry-europe.onlinelibrary.wiley.com/doi/10.1002/cctc.202400271 by Karlsruher Institut F., Wiley Online Library on [13/05/2024]. See the Terms and Conditions (https://onlinelibrary.wiley.com/terms-and-conditions) on Wiley Online Library for rules of use; OA articles are governed by the applicable Creative Commons License

formation observed at the collector electrode exhibits a distinct peak between the onset of the ORR and the onset of the HER region. Additionally, the curves for both scan directions are nearly reversible.

These results differ from those obtained on Ru(0001) electrodes mainly in the following features. First, the CVs for Ru(pc) in H_2SO_4 electrolyte do not show the pronounced inhibition of the ORR by $*HSO_4$ in the potential range between 0.0 and 0.25 V. Second, the complete inhibition of the ORR in the positive-going scan in the same electrolyte at potentials >0.25 V is missing as well. These differences are also reflected in the H_2O_2 formation. On the other hand, also on Ru(pc), the currents are lower in H_2SO_4 than in $HClO_4$ electrolyte, suggesting that the presence of (bi)sulfate species reduces the effective overall activity of the electrode.

We suggest that the differences in the reaction characteristics can be explained by the structural differences between the well-defined Ru(0001) on the one hand and Ru(pc) electrodes with their different surface sites and also much higher defect densities on the other hand. Based on the Sabatier principle, the abundance of different adsorption sites with different Ru–O/Ru–OH adsorption energies will lead to different reaction rates on different sites. Furthermore, different adsorption energies will also shift the regions of stable anion adsorption, which is crucial, e.g., for anion adsorption-induced reaction inhibition effects. Therefore, it is not surprising that i) the ORR activities differ for Ru(0001) and Ru(pc) and that ii) potential dependent inhibition effects, e.g., due to the presence of $*HSO_4$, are not well resolved or even hardly visible on the Ru(pc) sample.

In addition, different structural properties will also have an effect on the ORR selectivity (H_2O vs. H_2O_2 formation), which can be deduced from the yields. So far, H_2O_2 yields on Ru electrodes/catalysts were rarely reported in the literature, in particular not for single crystal electrodes. For carbon-supported Ru catalysts, Hara et al. reported H_2O_2 yields in the range of a few percent in 0.5 M H_2SO_4 for potentials <0.6 V, with an onset of the ORR at 0.7 V.[11] Bron et al. reported yields of approximately 22 % close to the onset potential of the ORR in 0.5 M H_2SO_4, which dropped to around 5 % close to the potential for hydrogen adsorption and evolution.[53] Similar values and trends were obtained for the Ru(pc) electrodes presented in Section S5 of the SI. Based on the pronounced differences in the yields reported so far for different types of Ru(pc)[11,53] and Ru(0001) single crystals (this work) substantiates the assumption that the selectivity strongly depends on the structural properties of the Ru electrode.

In total, the site averaging effects encountered on polycrystalline materials underline the importance and relevance of experimental studies using structurally well-defined single-crystal electrodes as reference systems for theoretical studies of the ORR, particularly for strongly binding metals such as Ru.

Conclusions

We revisited the ORR on Ru(0001) in O_2 saturated 0.1 M $HClO_4$ and 0.5 M H_2SO_4 to gain a better atomic-scale mechanistic understanding of the complex, potential-dependent reaction behavior, extending the potential range into the HER region. Using the results of our previous studies and assuming that the potential-dependent adlayer composition is similar in the absence and presence of O_2, we could demonstrate that the potential-dependent activity for both the ORR and the formation of H_2O_2 is closely related to the potential-dependent changes in the composition and structure of the adlayer. In both electrolytes, the onset of the ORR coincides with the onset of the partial reduction of the *O-dominated adlayer.

In $HClO_4$, the rate continuously increases with more negative potentials until saturating before the HER region. In the HER region, the current increases again, with ORR and HER occurring simultaneously. In the reverse scan, the rate is almost reversible. In contrast, in H_2SO_4, ORR is only active in regions where no blocking $*HSO_4$ is on the surface, i.e., in the negative-going scan between the onset of the ORR and -0.2 V and in the HER region. No reaction occurs in the positive-going scan at potentials above the HER. Significant H_2O_2 yields were observed in the potential region where surface *O is transformed into *OH (region II) in both electrolytes. Its formation is rationalized by an outer-sphere reaction mechanism, where hydrogen is transferred from the OH adlayer to the O_2 residing in the electrolyte above the electrode. In combination, these results demonstrate the enormous effects adsorbed species can have on the ORR reaction characteristics in general. Furthermore, the results of this work can serve as a perfect basis and reference system for further theoretical studies.

Experimental

The experiments were performed in a combined UHV[54] and electrochemistry setup, which has been described in detail elsewhere.[55]

Materials

The acid solutions were prepared from high-grade chemicals and MilliQ water (18.2 MΩ cm). We used H_2SO_4 Merck Suprapure 98 % and $HClO_4$ Merck Suprapure 70 %. The electrolytes were purged with N_2 (Westfalen 6.0) or O_2 (6.0, MTI) for the ORR measurements.

The Ru(0001) single crystal electrodes were purchased from MaTecK GmbH (purity 99.99 %, orientation accuracy $<0.1°$).

The glassware was cleaned before each experiment by storage in highly concentrated KOH overnight and subsequently thoroughly boiled in and rinsed with hot MilliQ water.

Sample Preparation

The Ru(0001) single crystal was prepared under UHV conditions according to previous reports.[34] The preparation involved Ar ion sputtering ($p_{Ar}=3\times10^{-5}$ mbar, $I=4$ μA cm^{-2}) for at least 15 minutes, subsequent cycles of flash annealing to 1600 K and adsorption of 10 L of O_2 (1 L: 10 s $p_{O_2}=1\times10^{-6}$ mbar) to remove carbon

© 2024 The Authors. ChemCatChem published by Wiley-VCH GmbH

18673899, 0, Downloaded from https://chemistry-europe.onlinelibrary.wiley.com/doi/10.1002/cctc.202400271 by Karlsruher Institut F., Wiley Online Library on [13/05/2024]. See the Terms and Conditions (https://onlinelibrary.wiley.com/terms-and-conditions) on Wiley Online Library for rules of use; OA articles are governed by the applicable Creative Commons License

impurities, and finally three flash annealing cycles to 1600 K (without dosing O_2). The quality of the surface of the electrodes was verified by STM measurements under UHV conditions.

Electrochemical Procedure

The electrochemical and -catalytic measurements were performed in a dual thin layer flow cell equipped with a Pt collector electrode in a second compartment at the electrolyte outlet.[55] The potential was controlled by a bipotentiostat (Pine Instruments, AFCBP-1). A Au wire served as a counter electrode, and a home-made reversible hydrogen electrode served as a reference electrode. Throughout this work, all potentials are referred to the RHE scale. During the ORR measurements, the potential of the collector electrode was set to 1.2 V versus the reversible hydrogen electrode (RHE), allowing for almost fully selective oxidation of H_2O_2 formed during the ORR. A detailed description of the cell design can be found elsewhere.[55]

For the electrochemical measurements, the freshly prepared Ru-(0001) single crystals were transferred into a load lock chamber that was flushed with N_2 until atmospheric pressure was reached. Subsequently, the electrode was mounted on the electrochemical flow cell, by pressing the electrode against the O-ring of the cell. The deaerated electrolyte was flown through the cell. Possible bubbles were removed from the electrolyte capillaries. Potential control can only be guaranteed after the complete removal of all bubbles. Consequently, the electrode was left at open circuit potential during this process, which took ca. 30 s. Then, several BCVs were recorded until the residual O_2 level in the electrolyte decreased so that the current in the double layer region (within region III) was almost symmetric on the current axis. Next, several BCVs with different scan rates and potential limits were recorded (the number varied between different measurements). Finally, the electrolyte was purged for 15 min with O_2, followed by several potential cycles (ORR-CVs) with different potential limits and scan rates.

CRediT

A.K. Engstfeld: Conceptualization, Software, Visualization, Supervision, Investigation, Formal Analysis, Writing – Original Draft Preparation, Data Curation. **S. Beckord**: Investigation. **S. Fuchs**: Investigation. **R.J. Behm**: Writing – Reviewing and Editing, Resources, Funding Acquisition.

Acknowledgements

This work was supported by the Deutsche Forschungsgemeinschaft (DFG) via the Research Unit 1376 (Be 1201/18-2) and by the Baden-Württemberg Stiftung via the Competence Network for Functional Nanostructures (FNV A1). We thank Z. Jusys for the fruitful discussions. Open Access funding enabled and organized by Projekt DEAL.

Conflict of Interests

The authors declare no conflict of interest.

Data Availability Statement

The data supporting the findings of this study are openly available in Zenodo at http://doi.org/10.5281/zenodo.10979477.

Keywords: cyclic voltammetry · electrocatalysis · hydrogen peroxide · ORR · Ruthenium · single crystals

[1] M. Shao, Q. Chang, J.-P. Dodelet, R. Chenitz, *Chem. Rev.* **2016**, *116*, 3594–3657.
[2] A. M. Gómez-Marín, E. A. Ticianelli, *Curr. Opin. Electrochem.* **2018**, *9*, 129–136.
[3] A. Kulkarni, S. Siahrostami, A. Patel, J. K. Nørskov, *Chem. Rev.* **2018**, *118*, 2302–2312.
[4] J. K. Nørskov, J. Rossmeisl, A. Logadottir, L. Lindqvist, J. R. Kitchin, T. Bligaard, H. Jonsson, *J. Phys. Chem. B* **2004**, *108*, 17886–17892.
[5] V. Climent, J. M. Feliu, *J. Solid State Electrochem.* **2011**, *15*, 1297.
[6] B. Grgur, N. Marković, P. Ross, *Can. J. Chem.* **1997**, *75*, 1465–1471.
[7] A. Kuzume, E. Herrero, J. M. Feliu, *J. Electroanal. Chem.* **2007**, *599*, 333–343.
[8] M. Maciá, J. Campina, E. Herrero, J. Feliu, *J. Electroanal. Chem.* **2004**, *564*, 141–150.
[9] M. Metikoš-Huković, R. Babić, F. Jović, Z. Grubač, *Electrochim. Acta* **2006**, *51*, 1157–1164.
[10] M. Bron, P. Bogdanoff, S. Fiechter, M. Hilgendorff, J. Radnik, I. Dorbandt, H. Schulenburg, H. Tributsch, *J. Electroanal. Chem.* **2001**, *517*, 85–94.
[11] Y. Hara, N. Minami, H. Itagaki, *Appl. Catal. A* **2008**, *340*, 59–66.
[12] N. Anastasijević, Z. Dimitrijević, R. Adžić, *Electrochim. Acta* **1986**, *31*, 1125–1130.
[13] S. Duron, R. Rivera-Noriega, P. Nkeng, G. Poillerat, O. Solorza-Feria, *J. Electroanal. Chem.* **2004**, *566*, 281–289.
[14] N. A. Anastasijević, Z. Dimitrijević, R. R. Adžić, *J. Electroanal. Chem. Interfacial Electrochem.* **1986**, *199*, 351–364.
[15] L. Nekrasov, E. Krushcheva, *Soviet Electrochemistry* **1967**, *3*, 138–143.
[16] N. Anastasijević, Z. Dimitrijević, R. R. Adžić, *Electrochim. Acta* **1992**, *37*, 457–464.
[17] J. Prakash, H. Joachin, *Electrochim. Acta* **2000**, *45*, 2289–2296.
[18] N. Ramaswamy, S. Mukerjee, *J. Phys. Chem. C* **2011**, *115*, 18015–18026.
[19] H. Inoue, S. Brankovic, J. Wang, R. Adžić, *Electrochim. Acta* **2002**, *47*, 3777–3785.
[20] S. Brimaud, A. Engstfeld, O. Alves, H. Hoster, R. J. Behm, *Top. Catal.* **2014**, *57*, 222–235.
[21] N. Marinkovic, M. Vukmirovic, R. Adzic, *Mod. Aspects Electrochem.* **2008**; Springer; pp 1–52.
[22] J. Zhang, M. B. Vukmirovic, Y. Xu, M. Mavrikakis, R. R. Adzic, *Angew. Chem.* **2005**, *117*, 2170–2173.
[23] A. U. Nilekar, Y. Xu, J. Zhang, M. B. Vukmirovic, K. Sasaki, R. R. Adzic, M. Mavrikakis, *Top. Catal.* **2007**, *46*, 276–284.
[24] S. Stolbov, *J. Phys. Chem. C* **2012**, *116*, 7173–7179.
[25] G. A. Tritsaris, J. K. Nørskov, J. Rossmeisl, *Electrochim. Acta* **2011**, *56*, 9783–9788.
[26] S. Sakong, D. Mahlberg, T. Roman, M. Li, M. Pandey, A. Groß, *J. Phys. Chem. C* **2020**, *124*, 27604–27613.
[27] M. Shao, P. Liu, J. Zhang, R. Adzic, *J. Phys. Chem. B* **2007**, *111*, 6772–6775.
[28] J. Jin, W. Lin, P. Christensen, *Phys. Chem. Chem. Phys.* **2008**, *10*, 3774–3783.
[29] O. Alves, H. Hoster, R. Behm, *Phys. Chem. Chem. Phys.* **2011**, *13*, 6010–6021.
[30] H. Hoster, R. Behm, *Fuel cell catalysis: a surface science approach* **2009**, *1*, 465.
[31] M. Mercer, H. E. Hoster, *Electrocatalysis* **2017**, *8*, 518–529.
[32] A. K. Engstfeld, S. Brimaud, R. J. Behm, *Angew. Chem. Int. Ed.* **2014**, *53*, 12936–12940.
[33] A. K. Engstfeld, J. Klein, S. Brimaud, R. J. Behm, *Surf. Sci.* **2015**, *631*, 248–257.
[34] A. K. Engstfeld, S. Weizenegger, L. Pithan, P. Beyer, Z. Jusys, J. Bansmann, R. J. Behm, J. Drnec, *Electrochim. Acta* **2021**, *389*, 138350.
[35] A. El-Aziz, L. Kibler, *Electrochem. Commun.* **2002**, *4*, 866–870.

© 2024 The Authors. ChemCatChem published by Wiley-VCH GmbH

18673899, 0, Downloaded from https://chemistry-europe.onlinelibrary.wiley.com/doi/10.1002/cctc.202400271 by Karlsruher Institut F., Wiley Online Library on [13/05/2024]. See the Terms and Conditions (https://onlinelibrary.wiley.com/terms-and-conditions) on Wiley Online Library for rules of use; OA articles are governed by the applicable Creative Commons License

[36] N. Marinković, J. Wang, H. Zajonz, R. Adžić, *J. Electroanal. Chem.* **2001**, *500*, 388–394.
[37] J. Wang, N. Marinković, H. Zajonz, B. Ocko, R. Adžić, *J. Phys. Chem. B* **2001**, *105*, 2809–2814.
[38] S. B. Scott, A. K. Engstfeld, Z. Jusys, D. Hochfilzer, N. Knøsgaard, D. B. Trimarco, P. C. Vesborg, R. J. Behm, I. Chorkendorff, *Catal. Sci. Technol.* **2020**, *10*, 6870–6878.
[39] L. A. Kibler, *Int. Society Electrochem.* **2003**, 1–55.
[40] M. T. Koper, *Electrochim. Acta* **2011**, *56*, 10645–10651.
[41] S. Sakong, A. Groß, *ACS Catal.* **2016**, *6*, 5575–5586.
[42] O. Vinogradova, D. Krishnamurthy, V. Pande, V. Viswanathan, *Langmuir* **2018**, *34*, 12259–12269.
[43] P.-C. Lu, C.-H. Yang, S.-L. Yau, M.-S. Zei, *Langmuir* **2002**, *18*, 754–762.
[44] W. Chen, L. W. Liao, J. Cai, Y.-X. Chen, *J. Phys. Chem. C* **2019**, *123*, 29630–29637.
[45] C. Zalitis, J. Sharman, E. Wright, A. Kucernak, *Electrochim. Acta* **2015**, *176*, 763–776.
[46] Z. Jusys, R. J. Behm, *ChemRxiv.* **2024**, https://doi.org/10.26434/chemrxiv – 2024–2061.
[47] L. Liu, H. Kim, J.-W. Lee, B. N. Popov, *J. Electrochem. Soc.* **2007**, *154*, A123.
[48] V. Viswanathan, H. A. Hansen, J. Rossmeisl, J. K. Nørskov, *J. Phys. Chem. Lett.* **2012**, *3*, 2948–2951.
[49] S. Yang, A. Verdaguer-Casadevall, L. Arnarson, L. Silvioli, V. Colic, R. Frydendal, J. Rossmeisl, I. Chorkendorff, I. E. Stephens, *ACS Catal.* **2018**, *8*, 4064–4081.
[50] N. Ramaswamy, S. Mukerjee, *Chem. Rev.* **2019**, *119*, 11945–11979.
[51] G. A. Kamat, J. A. Zamora Zeledón, G. K. K. Gunasooriya, S. M. Dull, J. T. Perryman, J. K. Nørskov, M. B. Stevens, T. F. Jaramillo, *Commun. Chem.* **2022**, *5*, 20.
[52] M. Luo, M. T. Koper, *Nature Catalysis* **2022**, *5*, 615–623.
[53] M. Bron, P. Bogdanoff, S. Fiechter, I. Dorbandt, M. Hilgendorff, H. Schulenburg, H. Tributsch, *J. Electroanal. Chem.* **2001**, *500*, 510–517.
[54] K. Kopatzki; Sauerstoffadsorption, Ph.D. thesis, University München, The address of the publisher, **1994**; An optional note.
[55] J. Schnaidt, S. Beckord, A. K. Engstfeld, J. Klein, S. Brimaud, R. J. Behm, *Phys. Chem. Chem. Phys.* **2017**, *19*, 4166–4178.

Manuscript received: February 7, 2024
Revised manuscript received: February 29, 2024
Accepted manuscript online: February 29, 2024
Version of record online: ■■, ■■

© 2024 The Authors. ChemCatChem published by Wiley-VCH GmbH

18673899, 0, Downloaded from https://chemistry-europe.onlinelibrary.wiley.com/doi/10.1002/cctc.202400271 by Karlsruher Institut F., Wiley Online Library on [13/05/2024]. See the Terms and Conditions (https://onlinelibrary.wiley.com/terms-and-conditions) on Wiley Online Library for rules of use; OA articles are governed by the applicable Creative Commons License

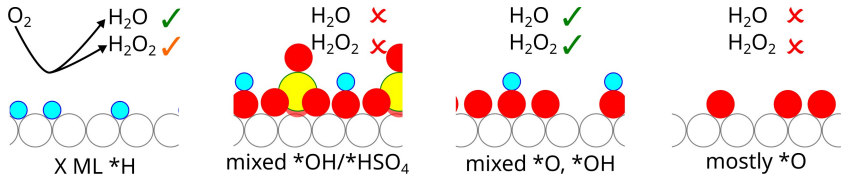

Classical mechanisms for the oxygen reduction reaction on metal electrodes require an adsobrate free surface. On the example of Ru single crystal electrodes, which are never free from adsorbates, we show that depending on the potential and electrolyte the reaction is either inhibited or can even lead to the formation of significant amounts of hydrogen peroxide.

A. K. Engstfeld, S. Beckord, S. Fuchs, R. J. Behm*

Impact of the Potential Dependent Surface Adlayer Composition on the ORR Activity and H_2O_2 Formation on Ru(0001) in Acid Electrolytes

18673899, 0, Downloaded from https://chemistry-europe.onlinelibrary.wiley.com/doi/10.1002/cctc.202400271 by Karlsruher Institut F., Wiley Online Library on [13/05/2024]. See the Terms and Conditions (https://onlinelibrary.wiley.com/terms-and-conditions) on Wiley Online Library for rules of use; OA articles are governed by the applicable Creative Commons License